Supporting Information:

Quantitative mechanical analysis of indentations on layered, soft elastic materials

Bryant L. Doss, Kiarash Rahmani Eliato, Keng-hui Lin, Robert Ros

Supplemental Table 1:

Hertz Model[1]:

$$f(r) = \frac{r^2}{2R}$$

$$\delta = \frac{{a_0}^2}{R}$$

$$F_0 = \frac{E_1}{(1 - v^2)} \frac{4}{3} \sqrt{R\delta^3}$$

Sneddon model[2]:

$$f(r) = r\cot\theta$$

$$\delta = \frac{1}{2} a_0 \pi \cot\theta$$

$$F_0 = \frac{E_1}{(1 - v^2)} \frac{2\delta^2}{\pi \cot\theta}$$

Hyberbolic model[3]:

$$f(r) = R\cot^2\theta \left[\sqrt{\frac{r^2}{(R\cot\theta)^2} + 1} - 1 \right]$$

$$\delta = \frac{a_0 \cot\theta}{2} \left[\frac{\pi}{2} + \tan^{-1} \left(\frac{a_0}{2R\cot\theta} - \frac{R\cot\theta}{2a_0} \right) \right]$$

$$F_0 = \frac{E_1}{(1 - v^2)} \frac{{a_0}^3}{R} \left\{ \left(\frac{R\cot\theta}{a_0} \right)^2 + \frac{R\cot\theta}{2a_0} \left[1 - \left(\frac{R\cot\theta}{a_0} \right)^2 \right] \left[\frac{\pi}{2} + \tan^{-1} \left(\frac{a}{2R\cot\theta} - \frac{R\cot\theta}{2a_0} \right) \right] \right\}$$

Sphero-conical model[4]:

$$b = R\cos\theta$$

$$f(r) = \begin{cases} R - \sqrt{R^2 - r^2},\ r \le b \\ (r-b)\cot\theta + R - \sqrt{R^2 - b^2},\ r > b \end{cases}$$

$$\delta = \begin{cases} \frac{a_0}{2} ln\left(\frac{R + a_0}{R - a_0}\right),\ a_0 \le b \\ a_0 ln\left(\frac{R + a_0}{\sqrt{R^2 - b^2} + \sqrt{{a_0}^2 - b^2}}\right) + a_0 \cos^{-1}\left(\frac{b}{a_0}\right)\cot\theta,\ a_0 > b \end{cases}$$

$$F_0 = \begin{cases} \frac{E_1}{(1-\nu^2)}\left[\frac{1}{2}\left({a_0}^2 + R^2\right) ln\left(\frac{R + a_0}{R - a_0}\right) - aR\right],\ a_0 \le b \\ \frac{E_1}{(1-\nu^2)}\left[\begin{matrix} {a_0}^2\cot\theta\cos^{-1}\frac{b}{a} + b\cot\theta\sqrt{{a_0}^2 - b^2} - a_0 R \\ + \sqrt{(R^2 - b^2)\left({a_0}^2 - b^2\right)} + {a_0}^2 \ln\left(\frac{R + a_0}{\sqrt{R^2 - b^2} + \sqrt{{a_0}^2 - b^2}}\right) \\ - \frac{R^2}{2}\ln\left(\frac{{a_0}^2 R^2 - \left(b^2 - \sqrt{(R^2 - b^2)\left({a_0}^2 - b^2\right)}\right)^2}{b^2 (R + a_0)^2}\right) \end{matrix}\right],\ a_0 > b \end{cases}$$

Supplementary Note 1: Approximation of integral transform method

We consider a system of two linearly elastic springs (k_1, k_2) in series undergoing compression of magnitude d on k_1 and d' on k_2 and with a fixed support on the k_2. Balancing the forces gives

$$d' = \frac{k_1 d}{k_1 + k_2} \tag{S1}$$

and the total force of compression on the system is

$$F = k_1\left(d - \frac{k_1 d}{k_1 + k_2}\right) \tag{S2}$$

Letting $F_0 = k_1 d/2$ represent the homogeneous case of k_1=k_2 and normalizing Eq. S2 gives

$$\frac{F}{F_0} = 1 - \frac{k_1 - k_2}{k_1 + k_2} = \frac{2}{\frac{k_1}{k_2} + 1} \tag{S3}$$

which may be rewritten as a hyperbolic tangent function with minor transformations of variables and constants. We find that this simple 1D model gives functionally similar results for scaling behavior of k_1/k_2 to E_1/E_2 in the full axisymmetric model of Dhaliwal and Rau, however the upper bounds of the model (when $E_1/E_2 \sim 0$) and the steepness of the sigmoidal transition differ depending on the characteristic length scale a_0/h of the indentation.

Therefore, in the case of an axisymmetric indentation into an axisymmetric elastic material, we phenomenologically modify Eq. S3 to include effects of the length scale in a power-law fashion as

$$\frac{F}{F_0}\left(\frac{a_0}{h},\frac{E_1}{E_2}\right)\rightarrow\frac{B\left(\frac{a_0}{h}\right)+1}{\left(\frac{E_1}{E_2}\right)^{A\left(\frac{a_0}{h}\right)}B\left(\frac{a_0}{h}\right)+1} \tag{S4}$$

Here, the functions *A* and *B* represent the steepness and the upper bounds of the sigmoidal transition, respectively, and both depend on the indentation length scale a_0/h. F/F_0=1 for E_1=E_2 and B=0 when a_0/h=0 resulting in F/F_0=1, thus the conditions of the homogeneous case are satisfied.

Fits for *A* and *B* were performed for all values of a_0/h ranging from 0.01 to 1.00. The weights of the least squares regression is related to the inverse of the value of F/F_0 and is higher for lower values of a_0/h. The force correction was calculated for a parabolic (Hertz model) indenter with radius for six orders of magnitude of E_1/E_2 and a_0/h up to 1.00 in increments of 0.01 (Fig. S2). For a given a_0/h, the force correction is calculated for all E_1/E_2. *A* and *B* were empirically fit in a least-squares manner to

$$A\left(\frac{a_0}{h}\right)\rightarrow\min\left(1,C_0+C_1\left(\frac{a_0}{h}\right)+C_2\left(\frac{a_0}{h}\right)^2\right) \tag{S5}$$

$$B\left(\frac{a_0}{h}\right)\rightarrow C_3\left(\frac{a_0}{h}\right)+C_4\left(\frac{a_0}{h}\right)^2 \tag{S6}$$

In this definition, the power law *A* cannot be less than zero nor greater than one, therefore the additional constraint of the minimum function is added. Fitting for the constants while assuming v_1 = v_2 = 0.5 gives

$$A\left(\frac{a_0}{h}\right)\approx 0.72-0.34\left(\frac{a_0}{h}\right)+0.51\left(\frac{a_0}{h}\right)^2 \tag{S7}$$

$$B\left(\frac{a_0}{h}\right) \approx 0.85\left(\frac{a_0}{h}\right) + 3.36\left(\frac{a_0}{h}\right)^2 \quad \text{(S8)}$$

It should be noted that the coefficients given in Eq. (S7-S8) do not represent corrective orders in the approximation as they do in other works[5-7], but rather they are determined simply by performing a least-squares regression over A and B.

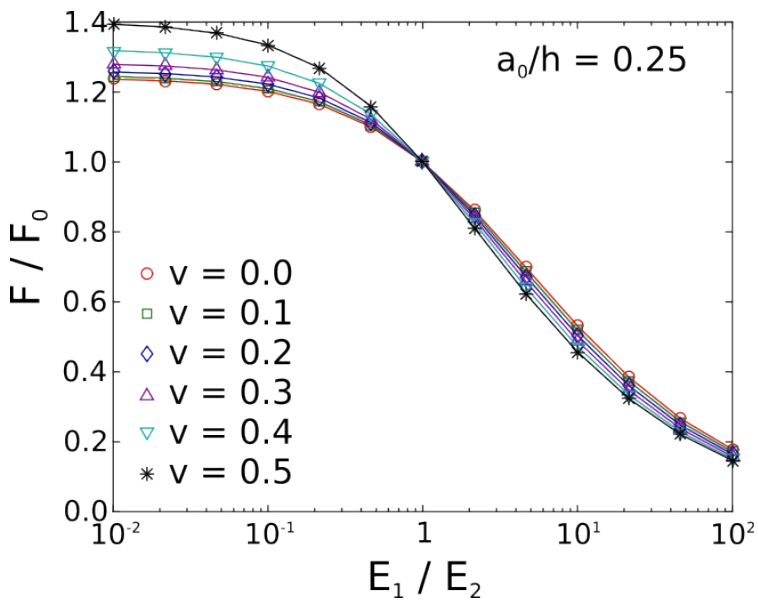

Fig. S1: Effect of the Poisson's ratio on indentations into layered systems using a parabolic (Hertz model) indenter. For all cases, $v = v_1 = v_2$.

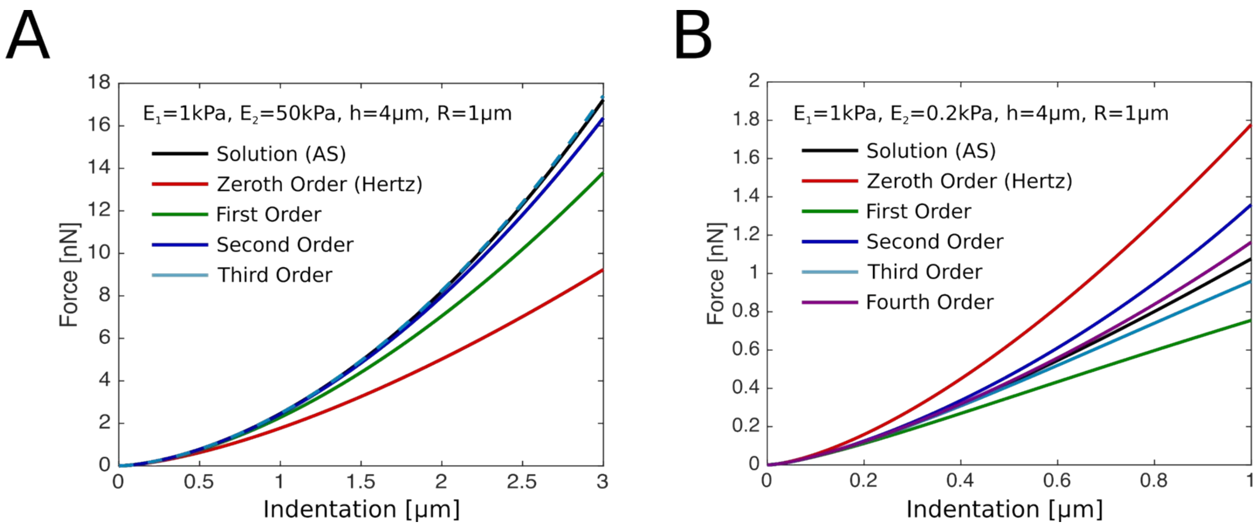

Fig. S2: Comparison of numeric solving methods for ϕ to determine F (Eq. 1-9) between Dhaliwal and Rau[8] (DR) and Atkinson and Shampine[9] (AS). (A) In the case of a stiff substrate and soft layer, black is AS numeric method and red, green, blue, and cyan represent DR method for different orders (zeroth, first, second, and third, respectively). (B) In the case of a soft substrate and stiff layer, black is AS numeric method and red, green, blue, cyan, and magenta represent DR method for different orders (zeroth, first, second, and third, respectively). Parameters are E_1=1 kPa, h=4 µm, R=1 µm, and (A) E_2=50 kPa and (B) E_2=0.2 kPa.

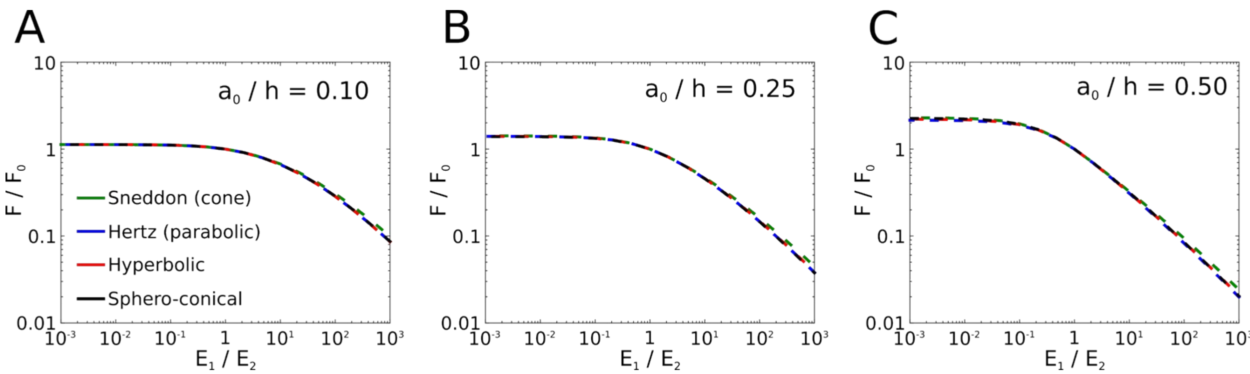

Fig. S3: Results of the numeric model. Log-log corrections to the force F/F_0 as a function of elasticity mismatch E_1/E_2 are shown for (A) a0/h=0.10, (B) a0/h=0.25, and (C) a0/h=0.50 for Hertz model (blue), Sneddon model (green), hyperbolic (red), and sphero-conical (black) indenter geometries.

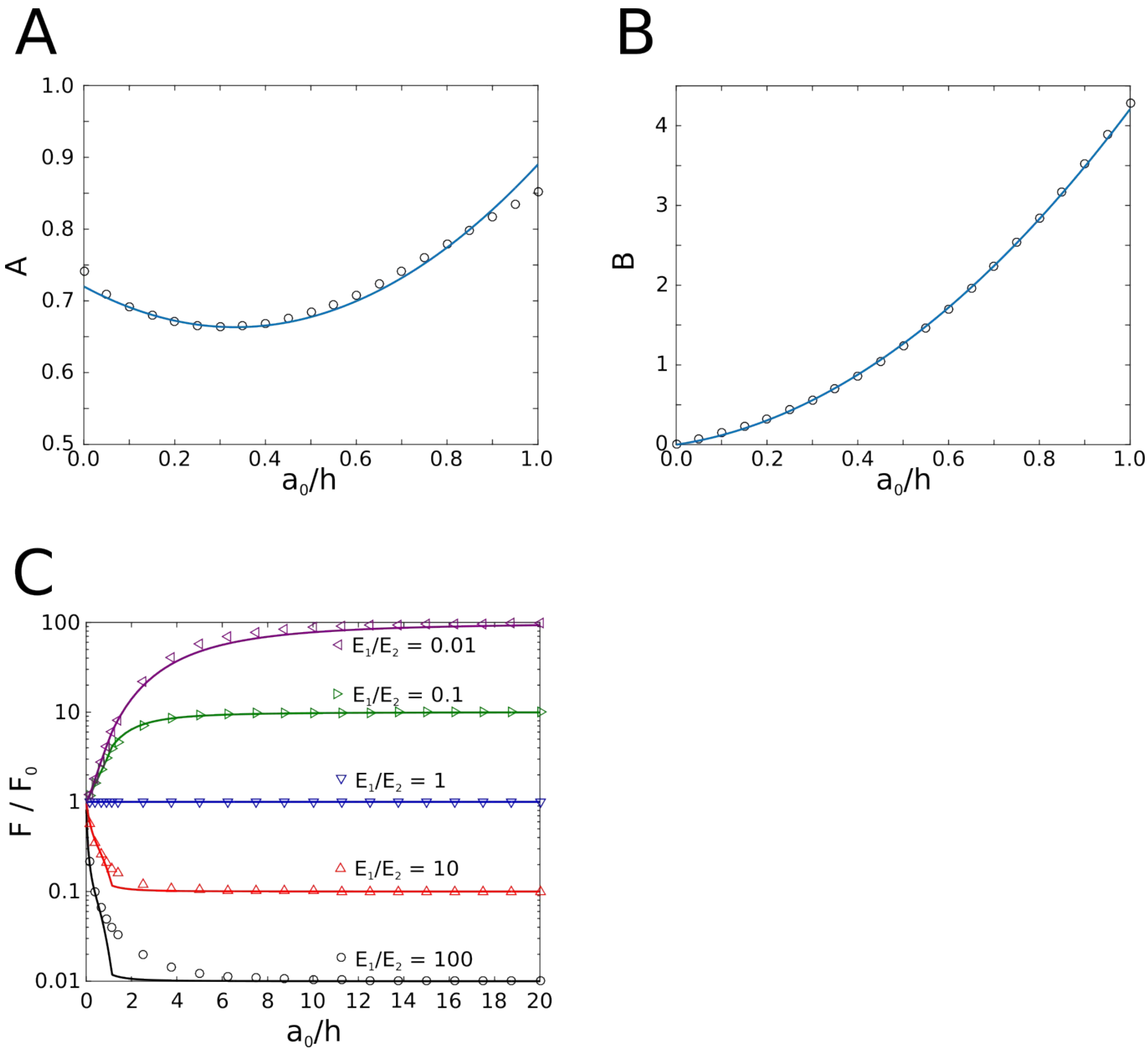

Fig. S4: Additional details of fitting to determine Eq. (14-15). (A) Values calculated for A as a function of a_0/h (black circles) and the corresponding fit to Eq. (S2) (blue lines). (B) Values calculated for B as a function of a_0/h (black circles) and the corresponding fit (blue lines). (C) F/F_0 as a function of a_0/h (larger values) for various values of E_1/E_2 (blue E_1/E_2=1, red 10, black 100, green 0.1, and magenta 0.01). Open markers indicate the solution to Eq. (1-9) while solid lines indicate the solution to Eq. (16).

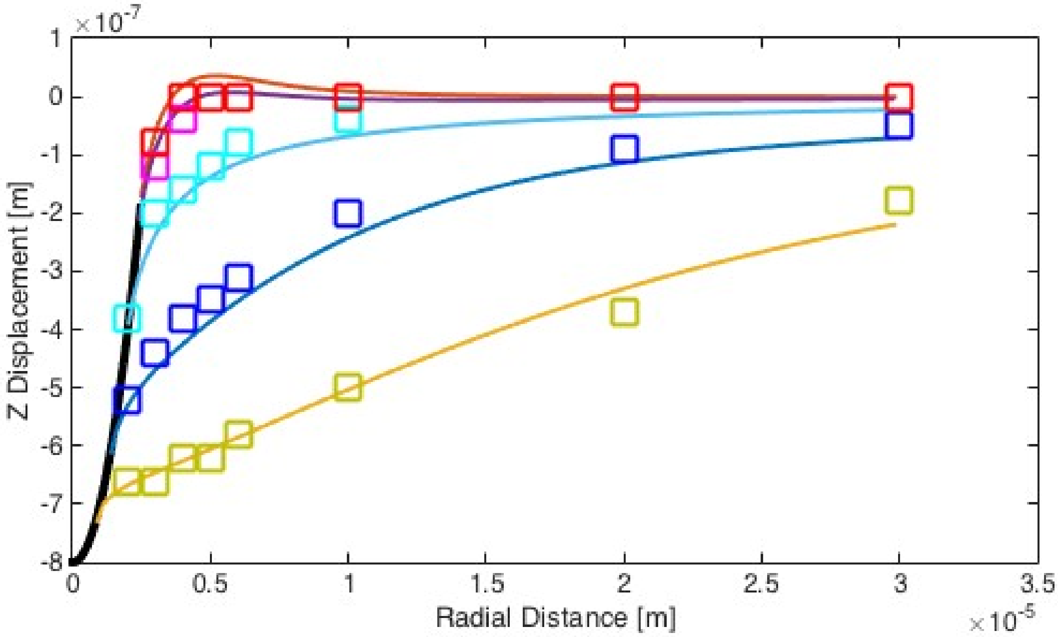

Fig. S5: Surface displacement profile of indentations into two-layered materials. Squares show results from finite element analysis and solid lines indicate theory Eq. (10). For all simulations, R=5 μm, δ=800 nm, E_1=100 kPa, h=4 μm, $\nu_1=\nu_2$=0.49, and E_2=10 MPa, 1 MPa, 100 kPa, 10 kPa, and 1 kPa for red, magenta, teal, blue, and yellow, respectively. The black curve indicates the shape of the indenting probe.

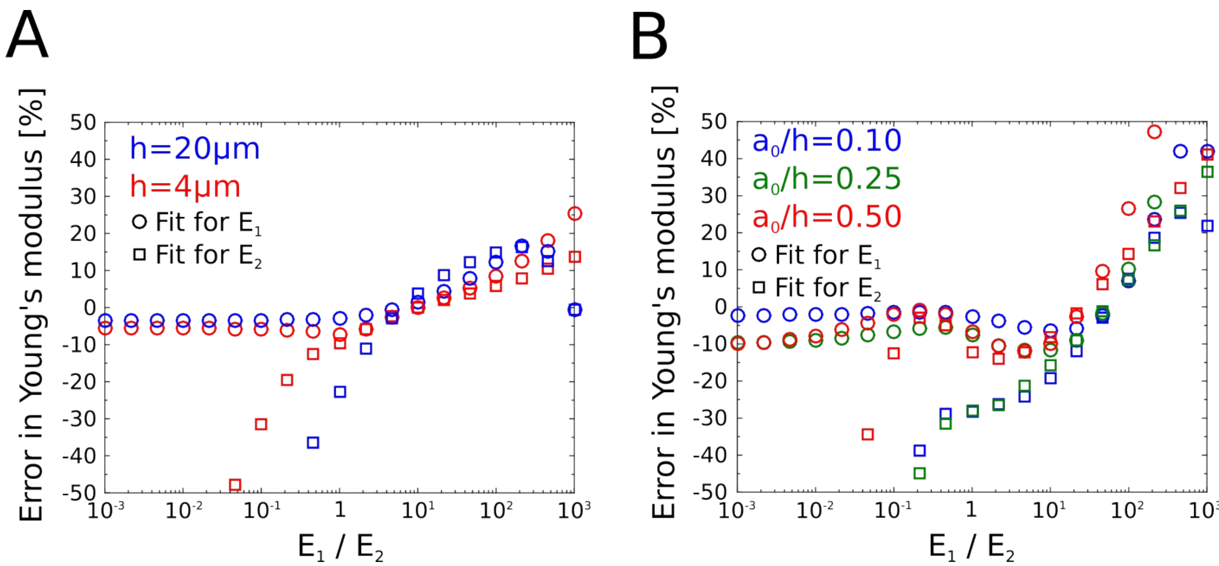

Fig. S6: Errors in deconvoluting Young's modulus from finite element simulations. (A) Numeric method solving Eq. (1-9), and (B) approximate method using Eq. (14). Points not shown if the absolute error is greater than 50%.

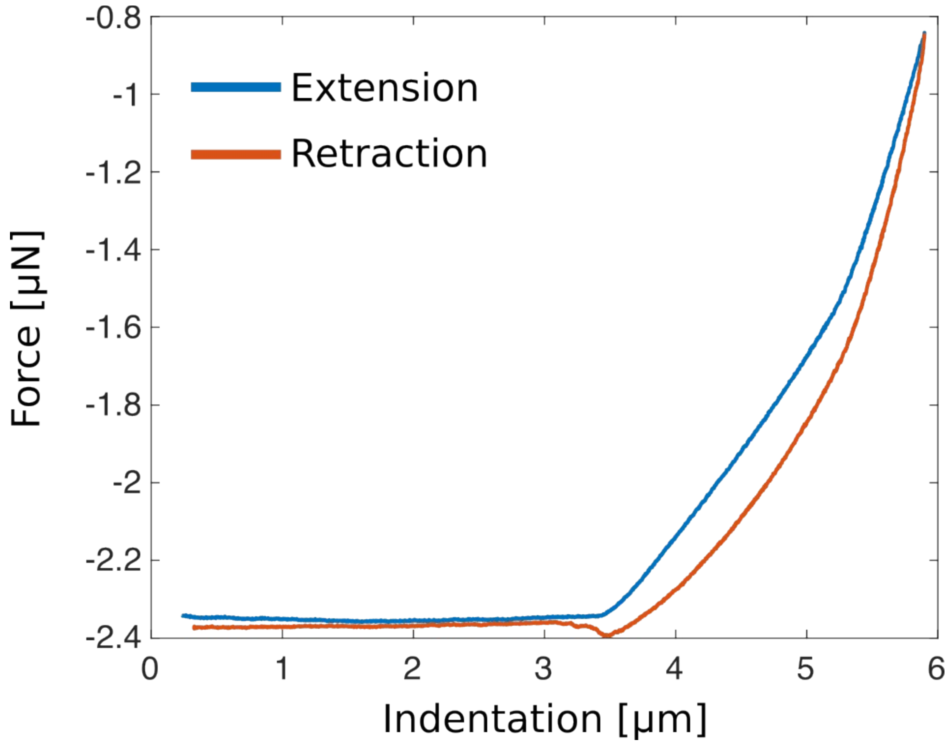

Fig. S7: Representative force-indentation curve on a thick layer of 40:1 PDMS. Blue shows the extension curve, red shows the retraction curve.

1. Hertz, H., *Uber die Beriihrung fester elastischer Korper.* J. Reine Angewandte Mathematik, 1882. **92**: p. 156-171.
2. Sneddon, I.N., *The relation between load and penetration in the axisymmetric boussinesq problem for a punch of arbitrary profile.* International Journal of Engineering Science, 1965. **3**(1): p. 47-57.
3. Akhremitchev, B.B. and G.C. Walker, *Finite Sample Thickness Effects on Elasticity Determination Using Atomic Force Microscopy.* Langmuir, 1999. **15**(17): p. 5630-5634.
4. Staunton, J.R., et al., *Correlating confocal microscopy and atomic force indentation reveals metastatic cancer cells stiffen during invasion into collagen I matrices.* Sci Rep, 2016. **6**: p. 19686.
5. Dimitriadis, E.K., et al., *Determination of elastic moduli of thin layers of soft material using the atomic force microscope.* Biophys J, 2002. **82**(5): p. 2798-810.
6. Garcia, P.D. and R. Garcia, *Determination of the Elastic Moduli of a Single Cell Cultured on a Rigid Support by Force Microscopy.* Biophys J, 2018. **114**(12): p. 2923-2932.
7. Gavara, N. and R.S. Chadwick, *Determination of the elastic moduli of thin samples and adherent cells using conical atomic force microscope tips.* Nat Nanotechnol, 2012. **7**(11): p. 733-6.
8. Dhaliwal, R.S. and I.S. Rau, *Axisymmetric Boussinesq Problem for a Thick Elastic Layer under a Punch of Arbitrary Profile.* International Journal of Engineering Science, 1970. **8**(10): p. 843-&.
9. Atkinson, K.E. and L.F. Shampine, *Algorithm 876: Solving Fredholm Integral Equations of the Second Kind in Matlab.* ACM Transactions on Mathematical Software, 2008. **34**(4).